Qeios

Modelling Skeletal Muscle Motor Unit Recruitment Contributions To Contractile Function: Part 3 - Substrate Oxidation of Phosphagen, Lipid and Carbohydrate Metabolism

Robert Robergs[1,2], Kartier Leo[1], Lucy Mulligan[1], Gerhard Nygaard[3], Julia Davies[1], Tyler Clarke[1], Justin Holland[1]

[1] School of Exercise and Nutrition Sciences, O Block, A Wing, Level 4, Room A420, Faculty of Health, Queensland University of Technology, Kelvin Grove, Queensland, 4059, Australia

[2] Faculty of Health Studies, Jan Evangelista Purkyne University, Velka Hradebni 424/13, 400 96, Usti nad Labem, Czech Republic.

[3] Department of Computer Science, Electrical Engineering and Mathematical Sciences, Western Norway University of Applied Sciences, Høgskulen på Vestlandet, Postbox 7030, 5020 Bergen, Norway.

Address for correspondence: Robert Robergs, School of Exercise and Nutrition Sciences, O Block, A Wing, Level 4, Room A420, Faculty of Health, Queensland University of Technology, Kelvin Grove, Queensland, 4059, Australia; Phone: +61 7 3138 0339; Email: rob.robergs@qut.edu.au

ORCID #s

Robert A. Robergs: 0000-0002-7741-8136

Gerhard Nygaard: 0000-0003-2349-4659

Justin Holland : 0000-0001-6393-4319

Julia Davies: 0009-0001-3828-8519

Lucy Mulligan: NA

Kartier Leo: NA

Tyler Clarke: NA

https://doi.org/10.32388/C0I8U0

Abbreviations

AK	Adenylate Kinase
ATP	Adenosine Triphosphate
ATP_{to}	Adenosine Triphosphate turnover
CHO-GLY	Carbohydrate Glycolytic
CHO-MR	Carbohydrate – Mitochondrial Respiration
CK	Creatine Kinase
CK-AK	Creatine Kinase - Adenylate Kinase
CrP	Creatine Phosphate
FFA	Free Fatty Acid
FA-MR	Fatty Acid – Mitochondrial Respiration
FT	Fast Twitch
g·L	gram per Litre
Hz	Hertz
min	minute
mmol.L	millimole per Litre
ST	Slow Twitch
VO_2max	Maximal Oxygen Consumption
VL	Vastus lateralis

Abstract

This study aimed to apply and expand a prior model of motor unit recruitment of the vastus lateralis muscle (VL) to explore theoretical motor unit-specific substrate oxidation. The model utilized repeated contractions of varied frequency and fraction of motor unit recruitment, and four different genetic expressions of motor unit proportions. The study applied prior modelled data of the vastus lateralis (VL) motor unit contractile power and turnover of adenosine triphosphate (ATPto) based on non-linear functions of estimated percentage contributions of different energy systems across various muscle fibre types and contraction frequencies. Using LabVIEW™ programming, the model then used the prior data of ATPto and known ATP_{to} coefficients for substrate oxidation for the energy systems of phosphagen, glycolytic, and mitochondrial respiration from fatty acid and carbohydrate to calculate total and fibre type (motor unit) specific creatine phosphate catabolism, glycogenolysis, glycolytic glucose oxidation, fatty acid oxidation in mitochondrial respiration, glucose oxidation in mitochondrial respiration, and lactate production. Results revealed that for the phosphagen system, substrate turnover was far larger than research-based expressions of decreasing concentrations of creatine phosphate and ATP. This is to be expected for modelled research involving temporal summation of metabolism. Creatine phosphate is continually broken down and partially replenished during low intensity exercise, with such partial replenishment sustained during more intense exercise thanks to the creatine kinase shuttle. For carbohydrate oxidation, mitochondrial respiration accounted for greatest substrate oxidation in type I, and I-IIa motor units, where glycolysis accounted for most substrate oxidation in type IIa, IIab and IIb motor units. Fatty acid oxidation was larger for lower motor unit recruitment conditions, and highest for type I-IIa and IIa motor units. This result is logical based on the larger net muscle fibre recruitment for contraction conditions necessitating progression to fast twitch motor units causing higher substrate oxidation. Such findings reinforce the need for more research on fibre type specific substrate oxidation during different exercise intensities and durations.

Keywords: Fibre type; Glycolysis; LabVIEW; Motor unit recruitment; Mitochondrial respiration

Introduction

Most research on the metabolic biochemistry of skeletal muscle during exercise has come from human muscle biopsy methodologies (1-4). This procedure involves an incision to be made through the skin, subcutaneous fat and muscle fascia which allows a biopsy needle to be inserted through this incision and into the inner regions of the underlying muscle of interest. Suction is applied to the needle and the mass of muscle that is forced into the needle is cut with an inner guillotine within the biopsy needle. The biopsy needle and the muscle sample it contains are then removed.

The muscle sample typically contains approximately 250-400 muscle fibres, though on average there are 405,000 muscle fibres in the human vastus lateralis (VL) muscle (5). Therefore, the muscle biopsy sample is a small random sample with an unknown contribution of the different muscle fibre types. The sample is then biochemically analysed for metabolites and enzyme activities, with no recognition of the fibre type proportionality, or their involvement in the prior muscle contractions. While there are methods for studying single muscle fibres from these biopsy specimens, with this method being able to reveal the fibre type of the fibre under investigation, this work has been relatively recent, is time consuming and expensive to complete, and not yet adequately pursued in the context of understanding in-vivo muscle biochemistry and substrate oxidation during exercise (1,6).

Since the early 1990s, more elaborate muscle fibre type classification methods have been pursued, with the most prominent being based on different genetic expressions of the structure of the myosin heavy chain (1,7). This approach involves the separation of individual fibres from muscle biopsy samples, with subsequent homogenising of each fibre and the exposure of each fibre solution to gel electrophoresis (7). As the amino acids that form the structure of proteins are negatively charged, the different amino acid structure of the myosin heavy chain between different fibre types causes them to migrate different distances during gel electrophoresis. Such procedures allow for the isolation of the different myosin heavy chain proteins and the resultant myosin heavy chain classification of slow twitch (ST) fibres as Type I and I-IIa, and fast twitch (FT) fibres to be categorised into Type IIa, IIab and IIb muscle fibre types (1,8,9). The Type-IIa, IIa and IIab fibres have also been classed as intermediate fibres because they possess characteristics (contractile velocity, force, metabolic capacities, fatiguability) that are intermediate between fast fibres and slow fibres (1). Table 1 identifies the differences in mechanical parameters of each fibre type of the human VL.

Table 1: Myosin heavy chain fibre types of the human vastus lateralis muscle and their comparative contractile features. Data were retrieved from Bottinelli et al. (1).

	Type I	Type I-IIa	Type IIa	Type IIa-IIb	Type IIb
Maximum shortening velocity ($sL \cdot s^{-1}$)	0.264 ± 0.089	0.521 ± 0.149	1.121 ± 0.361	2.139 ± 0.453	2.418 ± 1.497
Force-velocity relationship (no units)	0.032 ± 0.024	0.030 ± 0.017	0.063 ± 0.029	0.060 ± 0.016	0.072 ± 0.035
Specific tension ($kN \cdot m^2$)	43.77 ± 21.90	50.97 ± 14.78	60.64 ± 34.86	64.73 ± 14.48	61.84 ± 14.49
Cross-sectional Area (μm^2)	9278 ± 3496	8569 ± 3211	7922 ± 2845	5492 ± 1167	6294 ± 2159

$sL \cdot s^{-1}$ = fibre segment length per second

A motor unit is the basic unit of muscle contraction. It consists of an alpha motor nerve and all the skeletal muscle fibres it innervates, including the neuromuscular junctions between the neuron and the fibres. Within a motor unit, all the fibres are of relatively the same type, though Botinelli et al. (1,8) have shown tremendous variability in contractile and metabolic traits within specific fibre type categories. Nevertheless, based on the pH sensitive myosin ATPase method (10), the three main muscle fibre types are slow twitch oxidative (Type I), fast twitch oxidative (Type I-IIa, IIa) and fast twitch glycolytic (Type IIab, IIb).

Type I and I-IIa fibres contract relatively slowly and use aerobic respiration to completely oxidise fatty acids, amino acids and carbohydrate to produce their cellular ATP turnover. Type IIa and IIab fibres have fast contractions and moderate fatiguability because they contain moderate mitochondrial mass, which enables them to contribute to cellular ATP turnover through a mix of aerobic and anaerobic catabolism. Type IIb fibres have fast contractions and primarily use anaerobic glycolysis because they have a very low mitochondrial mass. Consequently, Type IIb fibres fatigue more quickly than the other fibre type categories, and there is a gradual increase in motor unit size ($fibres \cdot unit^{-1}$) from Type I through to Type IIb (11-13). Most skeletal muscles in a human contain all five fibre types (motor units), though in varying proportions based on genetics and the specific muscle of interest.

According to the “all or none” principle, when muscle contraction occurs, each motor unit recruited contracts maximally (14). This is because action potentials that reach the sarcolemma of each muscle fibre of a motor unit cause a maximal contraction in all the fibres of the motor unit. However, peak force from muscle fibres is known to vary depending on calcium availability, inorganic phosphate accumulation, and temporal summation. Nevertheless, the increases in muscle force production during contractions predominantly result from increasing motor unit recruitment. Furthermore, motor unit recruitment largely depends on the cell body size, meaning that the order in which recruitment occurs

is from smallest to largest (Type I through to IIb) (15). This is referred to as the size principle of motor unit recruitment (12).

Despite this fact, very little is known about the motor unit-by-motor unit changes in substrate oxidation during increasing exercise intensities because most methods used in prior research of skeletal muscle biochemistry have been based on mixed fibre samples that only provide a whole muscle view of energy catabolism. The inability to study the fibre type specific contributions to gross muscle catabolism has constrained our understanding of the contributions of the different motor units to substrate oxidation, such as for fatty acid oxidation (β-oxidation and mitochondrial respiration) and carbohydrate oxidation (glycolysis and mitochondrial respiration). Consequently, the purpose of this research was to use prior research and knowledge of cellular and whole-body markers of muscle metabolism to explore the more in depth understanding of the important roles of motor unit recruitment in changing skeletal muscle metabolism during increasing contractile power. To do this a prior model of the contraction of the VL (16) and its resulting ATP turnover during 3 min of repeated contractions of at different frequencies of contractions and proportions of motor unit recruitment (17) were retrieved and from this data computations of substrate oxidation were completed as explained in Methods.

Methods

Data for motor unit-by-motor unit recruitment and increasing contractile power ($J.s^{-1}$) were obtained from Mulligan et al. (16). This data was first converted to data on muscle ATP turnover (ATP_{to}) based on the cellular biochemical efficiency (40%), and in vivo free energy release of ATP hydrolysis (50 $kJ \cdot M^{-1}$) (18) and this data is reported elsewhere (17). Now that the cellular ATP_{to} data was known for each motor unit recruited, across four different genetic expressions of motor unit proportions (80-20, 60-40, 40-60, 20-80 % ST-FT, respectively), five frequencies of muscle contraction (0.5, 1, 1.5, 2, 2.5 Hz), and nineteen different percentages of motor unit recruitment (5% increments from 5-95%), the task for this study was to obtain data for the fibre type specific capacities for each of the combined creatine kinase and adenylate kinase reactions (CK-AK), carbohydrate oxidation through glycolysis (CHO-GLY), carbohydrate oxidation via mitochondrial respiration (CHO-MR), and fatty acid oxidation via mitochondrial respiration (FA-MR).

Before the model could be applied to the motor unit ATP_{to} data, the change in the percentage contribution to ATP_{to} for the metabolic pathways of the CK-AK, FA-MR, CHO-GLY, and CHO-MR energy systems, specific to each of the muscle fibre types, had to be devised. Further, this had to be done for contraction frequencies ranging from 0.5-3 Hz in 0.5 Hz increments. This data could not be retrieved from prior research given that such work has yet to be completed. Consequently, we devised

this change in metabolic pathway proportionality as best as we could from theoretical functions of these pathways, knowledge of muscle cellular biochemistry, and prior research from whole muscle sample methods (1,4,19-24).

The formulation of substrate metabolic pathway relative contributions to ATP_{to} were first compiled in a spreadsheet software application (Excel™, Microsoft Corporation, Seattle, USA). Once the percentage contributions across the energy systems of the different fibre types and contraction frequencies were devised to sum to 100 ± 1 % across each metabolic pathway x Hz condition, the data were imported into a commercial graphics and curve fitting program (Prism v10.0.3, GraphPad Software LLC, Boston, USA). Calculations from curve-fitting were again checked and adjusted as necessary to sum to 100 ± 1 % across each metabolic pathway x Hz condition. The resulting non-linear functions are presented graphically in Results and Equations 1-20.

New LabVIEW programming was completed to allow a step-by-step process for calculating the ATP_{to} from each different energy system for the different genetic expressions and repeated contractions as previously identified. The nonlinear function equations for percentage ATP_{to} of the different energy systems across the muscle fibre types and contraction frequencies were applied to the motor unit recruitment ATP_{to} data. As this data was for individual motor units, each row entry was added to the prior row to result in an array of progressively summed incremental motor unit data for each metabolic pathway. Separate data files were processed for the four genetic expressions of motor unit proportions, the five different frequencies of muscle contraction, and the nineteen different percentage motor unit recruitment conditions.

Added computations in this program divided the ATP_{to} of each pathway by the ATP yield coefficients from each pathway to calculate the millimole (mmol) substrate oxidation. The ATP coefficients for the phosphagen, fatty acid oxidation, carbohydrate-glycolysis, and carbohydrate-mitochondrial respiration were 1.1, 129, 3, and 34, respectively. The resulting data file presented separate columns of individual incremental (summative) motor unit data for ATP_{to}, and substrate oxidation for each metabolic pathway expressed as $mmol \cdot L^{-1}$ and $g \cdot L^{-1}$, where the rows were the incremental motor unit recruitment data values.

The prior ATP_{to} data used to research the substrate turnover of this study was already coded to identify each sequential (row-by-row) motor unit type (1-5 for I, I-IIa, IIa, IIab, IIb, respectively). To acquire the metabolic substrate turnover data from each motor unit type, the motor unit type data from each row of the summed ATP_{to} data was used to code the new row delta increment in each ATP_{to} and substrate category. The array of data was then partitioned into data for each motor unit code and summed to reveal the ATP_{to} and substrate/pathway turnover for each metabolic pathway. Lactate

production was assumed to equal the difference in substrate turnover between CHO-GLY and CHO-MR. As such, the accumulation of glycolytic intermediates was not factored into the model as this would only amount to approximately 10 to 15 mmol·L^{-1} for the highest intensity contractions, with added complications for how this would differ between the muscle fibres of the different motor unit categories.

Mathematical Computations

Metabolic Pathway Non-linear Functions

The non-linear functions for the different metabolic pathways presented in Figure 2 were obtained from a commercial data analysis program (Prism V10, Graphpad software, Boston Massachusetts, USA). The equations for each function are presented below grouped by metabolic pathway for the different skeletal muscle fibre types, where the x-axis variable is contraction frequency.

CK-AK Type I

$$\%\ contribution = 2.031 * e^{0.5356x} \quad \text{Equation 1}$$

CK-AK Type I-IIa

$$\%\ contribution = 2.343 * (1.339x) + (1.373x^2) + (-0.4673x^3) + (0.1350x^4) \quad \text{Equation 2}$$

CK-AK Type IIa

$$\%\ contribution = 2.541 * e^{0.8839x} \quad \text{Equation 3}$$

CK-AK Type IIab

$$\%\ contribution = 5.618 * (-3.970x) + (9.721x^2) + (-4.256x^3) + (0.9696x^4) \quad \text{Equation 4}$$

CK-AK Type IIb

$$\%\ contribution = 5.274 * (10.35x) + (-8.939x^2) + (3.616x^3) \quad \text{Equation 5}$$

CHO-GLY Type I

$$\%\ contribution = 42.55 - 0.1682 \Big/ \left(1 + \left(2^{(1/1.318)-1}\right) \times \left(\left(1.591/x\right)^{5.375}\right)\right)^{1.318} \quad \text{Equation 6}$$

CHO-GLY Type I-IIa

$$\%\ contribution = 4.288 + (44.04 - 4.288) \Big/ \left(1 + 10^{((1.002-x) \times 1.587)}\right) \quad \text{Equation 7}$$

CHO-GLY Type IIa

$$\%\ contribution = 8.774 + {(57.97 - 8.774)}/{\left(1 + 10^{((0.9983 - x) \times 2.048)}\right)}$$ Equation 8

CHO-GLY Type IIab

$$\%\ contribution = 18.54 * (-18.13x) + (103.4x^2) + (-86.62x^3) + (28.96x^4) + (-3.509x^5)$$

Equation 9

CHO-GLY Type IIb

$$\%\ contribution = 12.09 * (85.42x) + (-65.49x^2) + (27.91x^3) + (-5.497x^4) + (0.1986x^5)$$

Equation 10

CHO-MR Type I

$$\%\ contribution = -21.67 + \left({((70.15 + 21.67) \times 0.7571)}/{1 + \left({1.134}/{x}\right)^{13.06}}\right) +$$

$$\left(\left({((70.15 + 21.67) \times (1 - 0.7571))}/{1 + \left({2.073}/{x}\right)^{-7.217}}\right)\right)$$ Equation 11

CHO-MR Type I-IIa

$$\%\ contribution = -32.73 + \left({((86.50 + 32.73) \times 0.5868)}/{1 + \left({0.7625}/{x}\right)^{4.633}}\right) +$$

$$\left(\left({((86.50 + 32.73) \times (1 - 0.5868))}/{1 + \left({1.352}/{x}\right)^{-3.323}}\right)\right)$$ Equation 12

CHO-MR Type IIa

$$\%\ contribution = 42.64 * (-151.3x) + (532.4x^2) + (-642.5x^3) + (351.0x^4) +$$

$$(-90.23x^5) + (8.873x^6)$$ Equation 13

CHO-MR Type IIab

$$\%\ contribution = -322.6 + \left({((67.9 + 322.6) \times 0.06076)}/{1 + \left({0.4074}/{x}\right)^{3.777}}\right) +$$

$$\left(\left({((67.9 + 322.6) \times (1 - 0.06076))}/{1 + \left({12.02}/{x}\right)^{-1.164}}\right)\right)$$ Equation 14

CHO-MR Type IIb

$$\%\ contribution = 41.44 * (98.29x) + (-269.5x^2) + (271.4x^3) + (-137.5x^4) + (34.47x^5) + (-3.389x^6)$$ Equation 15

FA-MR Type I

$$\%\ contribution = 0.6531 + {(97.94 - 0.6531)}\Big/{\left(1 + 10^{((1.181-x) \times -3.464)}\right)}$$ Equation 16

FA-MR Type I-IIa

$$\%\ contribution = 0.03365 + {(77.62 - 0.03365)}\Big/{\left(1 + 10^{((0.7409-x) \times -2.695)}\right)}$$ Equation 17

FA-MR Type IIa

$$\%\ contribution = -0.1147 + {(58.27 + 0.1147)}\Big/{\left(1 + 10^{((0.7106-x) \times -2.646)}\right)}$$ Equation 18

FA-MR Type IIab

$$\%\ contribution = -494.1 + \left({((528.9 + 494.1) \times 0.5171)}\Big/{1 + \left({0.7368}/{x}\right)^{-2.998}}\right) + \left(\left({((528.9 + 494.1) \times (1 - 0.5171))}\Big/{1 + \left({0.7605}/{x}\right)^{3.027}}\right)\right)$$ Equation 19

FA-MR Type IIb

$$\%\ contribution = (49.97 \times e^{7.292x}) + 0.01422$$ Equation 20

Equations 1-20 were then applied to the individual motor unit ATP_{to} data across the total motor unit pool for each of the five different motor unit genetic expressions based on select repeated contraction conditions. As previously explained, the contraction conditions consisted of 3 min of total duration for the five different contraction frequencies and 17 different fractional recruitment conditions. For example, the programming of the model was set to 0.5 Hz, and for this frequency the model then sequentially calculated the substrate turnover of each energy system of each motor unit using equations 1-20 based on coding for the type of motor unit. The data for each condition (frequency for a given fractional recruitment; 5 x 19 = 95) were saved separately as .txt files and consisted of data for the number of ATP regenerated from each pathway for each motor unit recruited. These files were then retrieved in the model and used

to apply the pathway specific ATP coefficients to calculate substrate oxidation as depicted in Equation 21 for each motor unit recruited.

$$Motor\ Unit\ Substrate\ Oxidation\ (mmol.L^{-1}) = {}^{ATPto}/_{Substrate\ ATP\ coefficient}$$

Equation 21

Pathway and motor unit type total substrate oxidation for given contraction conditions were calculated by simple summation across the specific motor unit types and/or metabolic pathways.

Results

Examples of the motor unit contractile power data and ATPto used to develop the model are presented in Figures 1a, b and Tables 1 and 2. The following process for the model was to develop the percentage contributions of the four different muscle energy systems with increases in contraction frequency. As explained in methods, this was based as much as possible on evidence from within cellular biochemistry and related research of changing energy system contributions to different intensities of muscle contraction. As prior research has been constrained to whole muscle or mixed fibre type sampling (not based on individual motor units or the metabolic differences between the fibre types of different motor unit categories) (1-4), such proportional representation of fibre type specific energy system contributions is unique. It is also critical to re-emphasise that this data was expressed to contraction frequency because, as governed by the All or None Principle, the muscle fibres of recruited motor units always contract maximally.

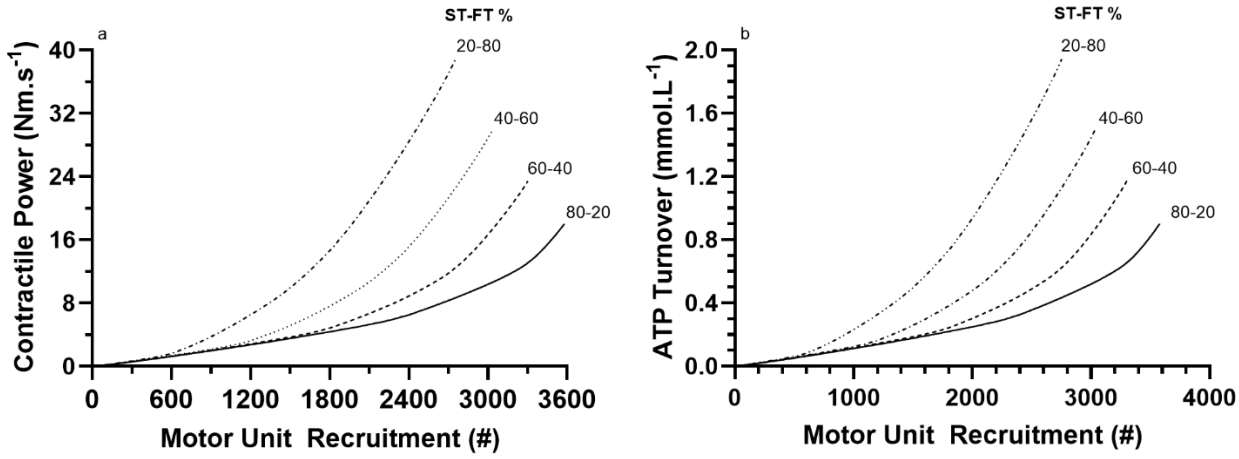

Figure 1: The data retrieved from prior model research from Parts-1 and -2 of this series for increases in a) contractile power (16) and b) increased muscle ATP_{to} (17) for increasing motor unit recruitment for the four different genetic expressions of motor unit proportionality.

Table 2: Data for the ATP_{to} of single muscle fibres and different motor unit sizes for each of the fibre type categories.

Motor Unit Type		Fibre	Motor Unit	
		ATP_{to}*	ATP_{to}^	Fibre #
ST	**I**	0.3293	0.027992	85
	I-IIa	0.4702	0.048003	102
FT	**IIa**	0.9160	0.109004	119
	IIab	1.0744	0.148269	138
	IIb	1.4000	0.214195	153

*ATP_{to} = $\mu M \cdot L^{-1}$; ^ATP_{to} = $mM \cdot L^{-1}$; Note, fibre differences are due to force differences between fibre types and the related motor unit sizes; # = predetermined motor unit sizes within the model.

Figure 2a-e presents the assumed percentage changes for the four energy systems for each of the five muscle fibre types. Note the decreased involvement of fatty acid oxidation with increasing contraction frequency and progression from Type I to IIb muscle fibres. In contrast, there is the expected increased dependence on carbohydrate oxidation and creatine phosphate degradation with increasing contraction frequency and recruitment progression from Type I to IIb motor units.

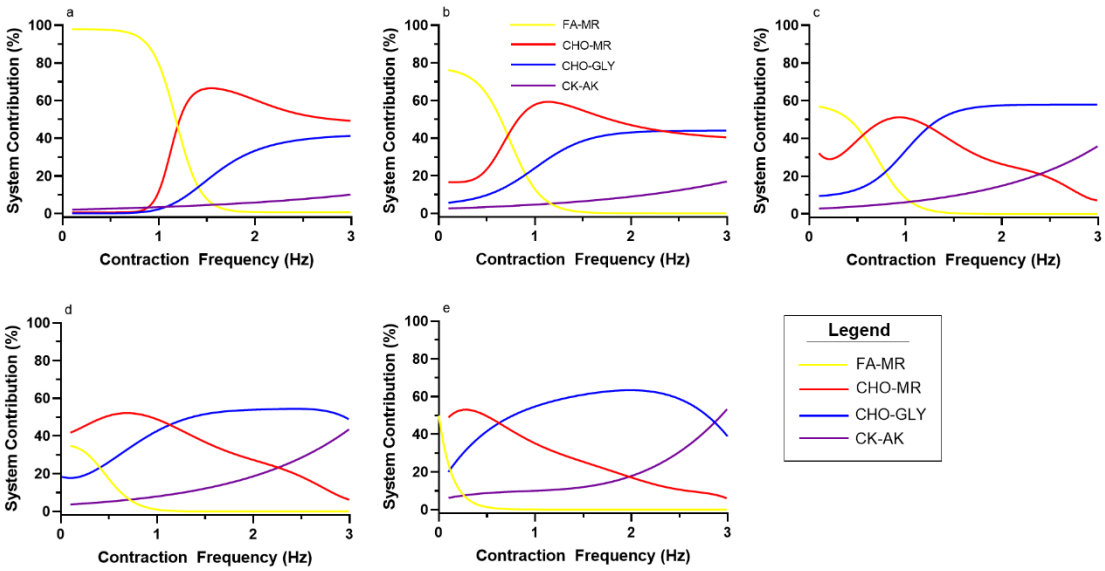

Figure 2: The % contribution of the different energy systems (see legend of 1b) across contraction frequencies of 0.5-3 Hz for the different muscle fibre types; a) Type I, b) Type I-IIa, c) Type IIa, d) Type IIab, e) Type IIb.

Based on the imported motor unit ATP_{to} data for different muscle contraction rates and percentage motor unit recruitment, the model then used the ATP yield per substrate flux to calculate substrate oxidation for each energy system. Correcting the energy pathway ATP_{to} calculations by the energy system ATP coefficients yielded the $mmol \cdot L^{-1}$ substrate oxidation of each energy system (Equation 21). Figure 3a-d presents this data across 0.05 to 0.95 fractional motor unit recruitment for 3 mins of repeated contractions ranging from 0.5-2.5 Hz for the CK-AK system. This was repeated for the FA-MR (Figure 4 a-d), CHO-GLY (figure 5 a-d) and CHO-MR (Figure 6 a-d) systems.

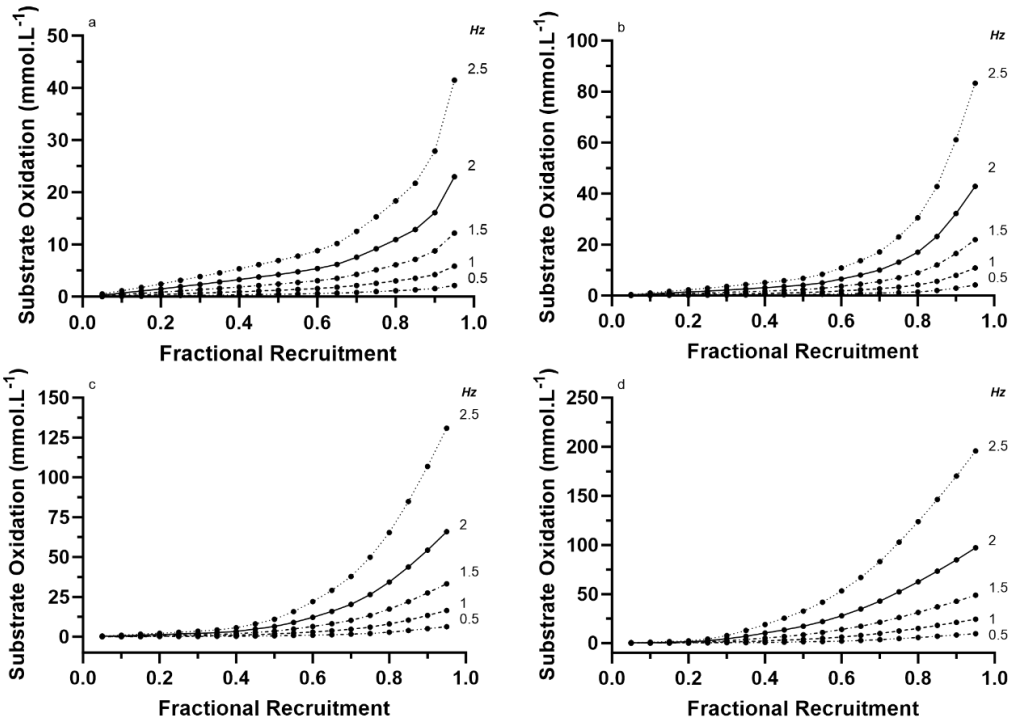

Figure 3: The total substrate oxidation for the CK-AK energy system across 0.05-0.95 fractional motor unit recruitment for 3 min of repeated contractions across 0.5-2.5 Hz for genetic motor unit expressions (ST-FT) of a) 80-20, b) 60-40, c) 40-60, d) 20-80 %, respectively.

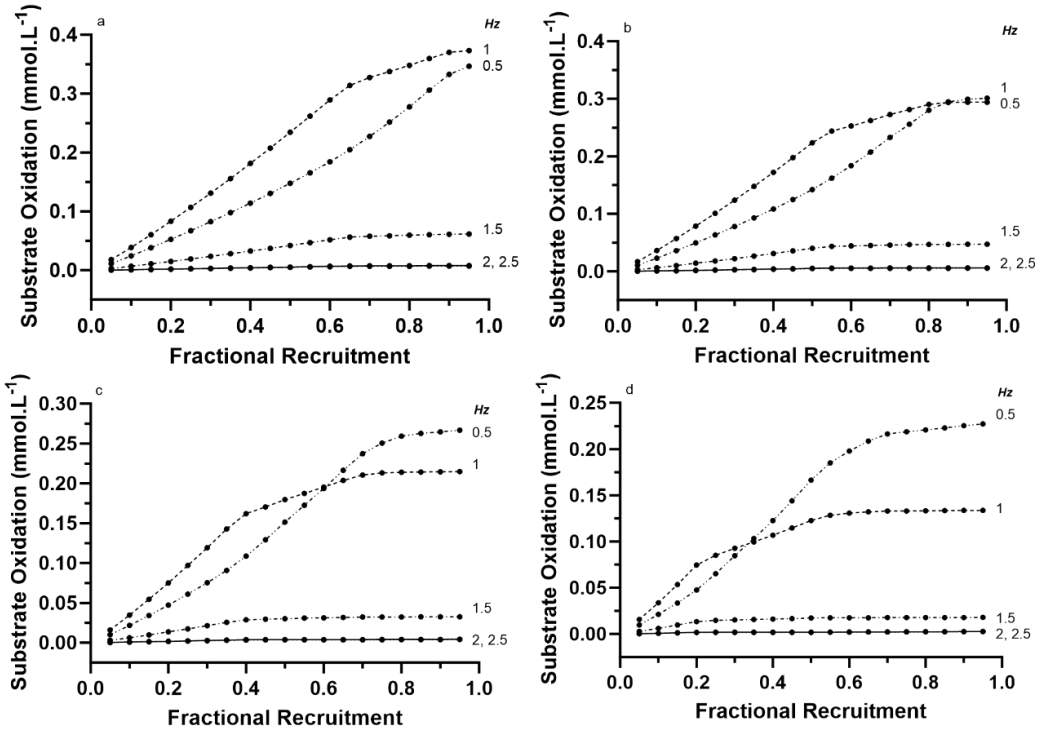

Figure 4: The total substrate oxidation for the FA-MR energy system across 0.05-0.95 fractional motor unit recruitment for 3 min of repeated contractions across 0.5-2.5 Hz for genetic motor unit expressions (ST-FT) of a) 80-20, b) 60-40, c) 40-60, d) 20-80 %, respectively.

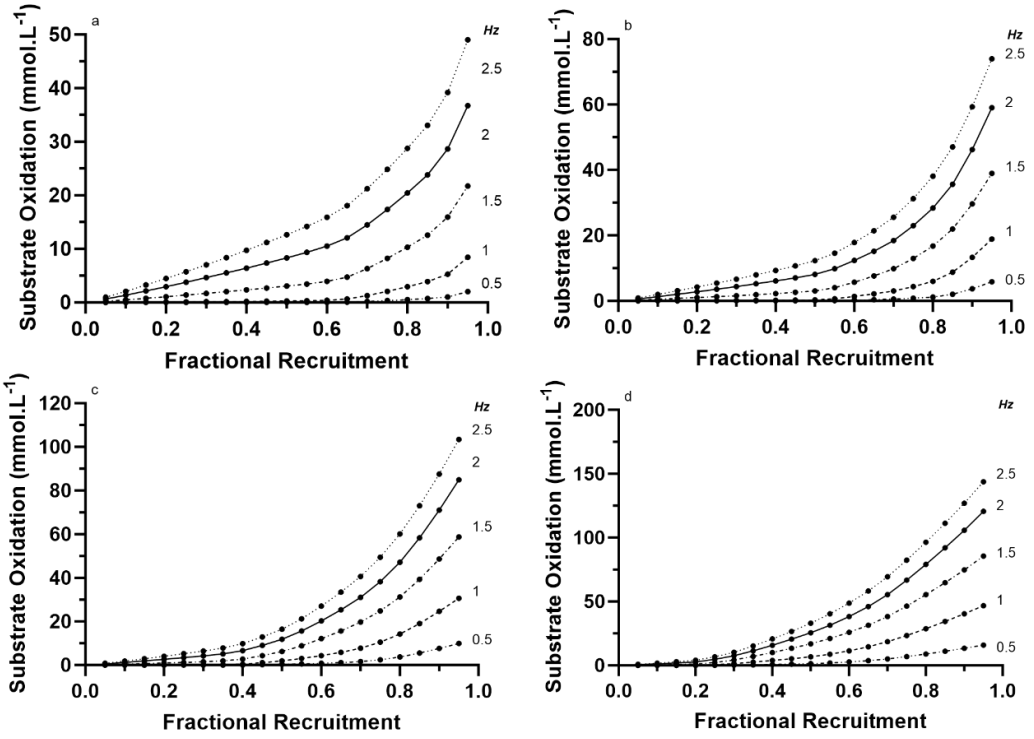

Figure 5: The total substrate oxidation for the CHO-GLY energy system across 0.05-0.95 fractional motor unit recruitment for 3 min of repeated contractions across 0.5-2.5 Hz for genetic motor unit expressions (ST-FT) of a) 80-20, b) 60-40, c) 40-60, d) 20-80 %, respectively.

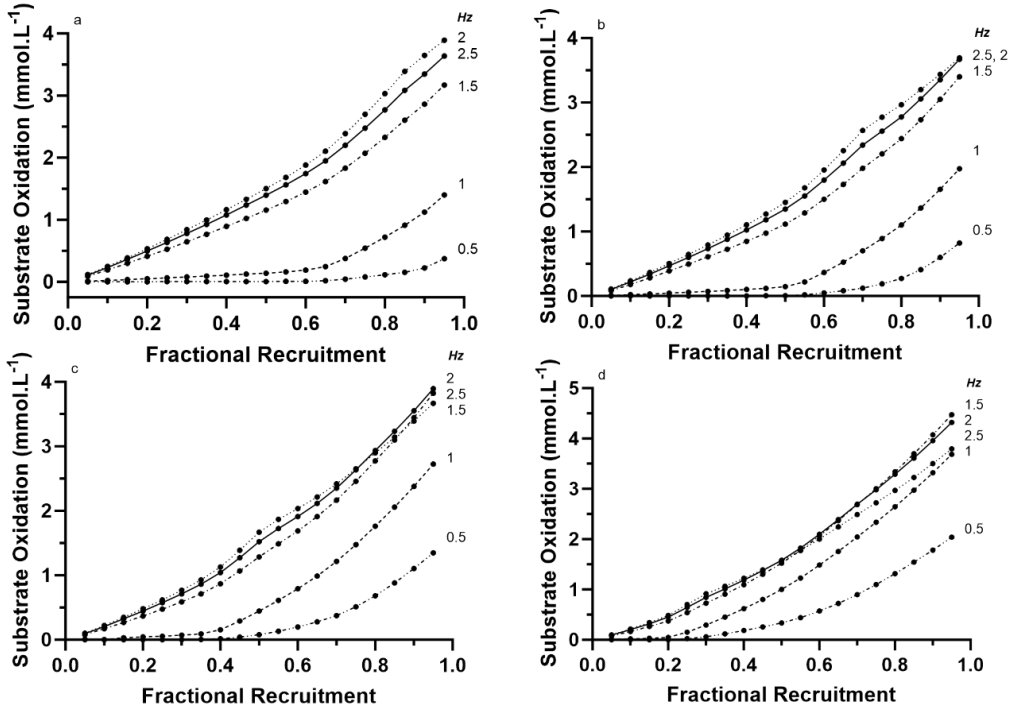

Figure 6: The total substrate oxidation for the CHO-MR energy system across 0.05-0.95 fractional motor unit recruitment for 3 min of repeated contractions across 0.5-2.5 Hz for genetic motor unit expressions (ST-FT) of a) 80-20, b) 60-40, c) 40-60, d) 20-80 %, respectively.

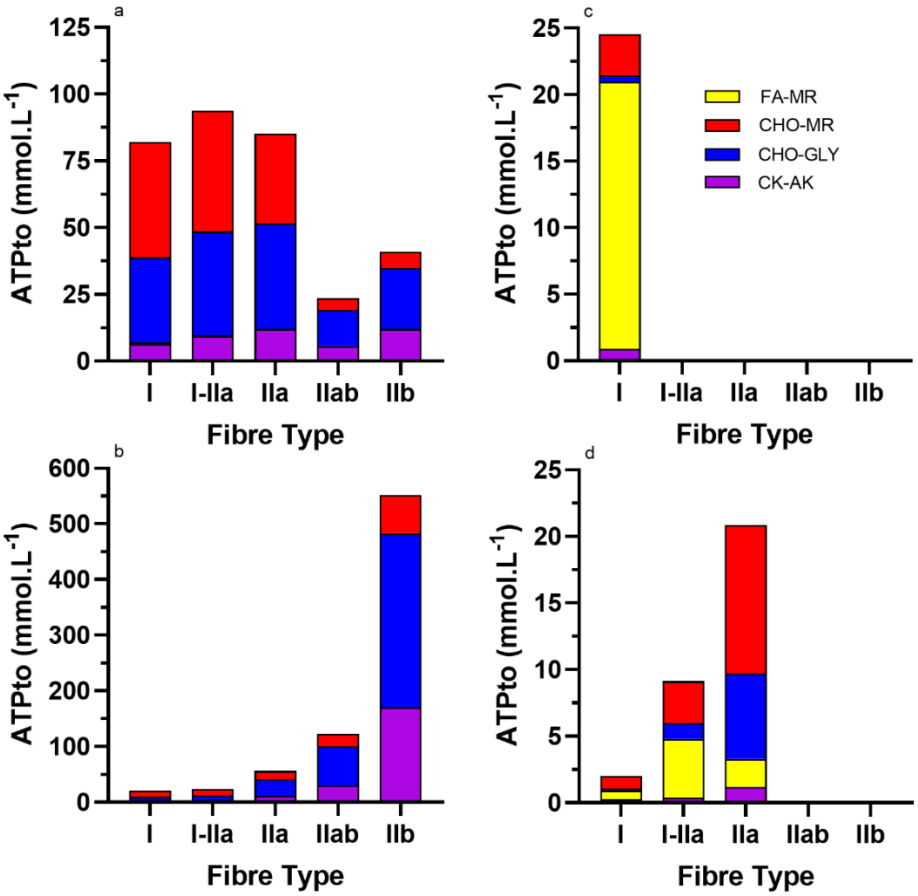

Figure 7: The metabolic pathway specific ATP_{to} for the different muscle fibre types for the contraction condition of 2.5 Hz and 95% motor unit recruitment for a) 80-20 and b) 20-80 % ST-FT, respectively. To document the difference to lower intensity muscle contractions, the ATP_{to} from the different metabolic pathways are presented for the contraction conditions of 1 Hz and 35% motor unit recruitment for c) 80-20 and d) 20-80 % ST-FT, respectively. The figure legend of c) applies to all figure subsets.

Figure 7 presents the metabolic pathway specific ATP_{to} data for each muscle fibre type for the two extremes of genetic motor unit expression and two different contraction conditions. As the data for Figure 7a,b is based on near maximal recruitment at the highest frequency of repeated muscle contraction, it is phosphagen and carbohydrate (glycolytic and mitochondrial respiration) dependent. The lower frequency and percent recruitment conditions had much higher contributions from fatty acid oxidation, as shown in Figure 7c,d. The higher FT expression of Figures 7b,d further documents the importance of motor unit recruitment and genetic expression, as well as the higher substrate turnover of fast twitch motor units due to their larger size and resultant power output and biochemical energy turnover.

The data for muscle lactate production are presented in Figure 8a-d. As explained in Methods, for the model, lactate production was the difference between substrate oxidation for CHO-GLY and CHO-MR. As to be expected based on data from Figure 2, the data of Figure

7 reveal that lactate production was meagre for slow twitch expressed muscle of the VL across all contraction frequencies, but considerable for fast twitch expressed muscle.

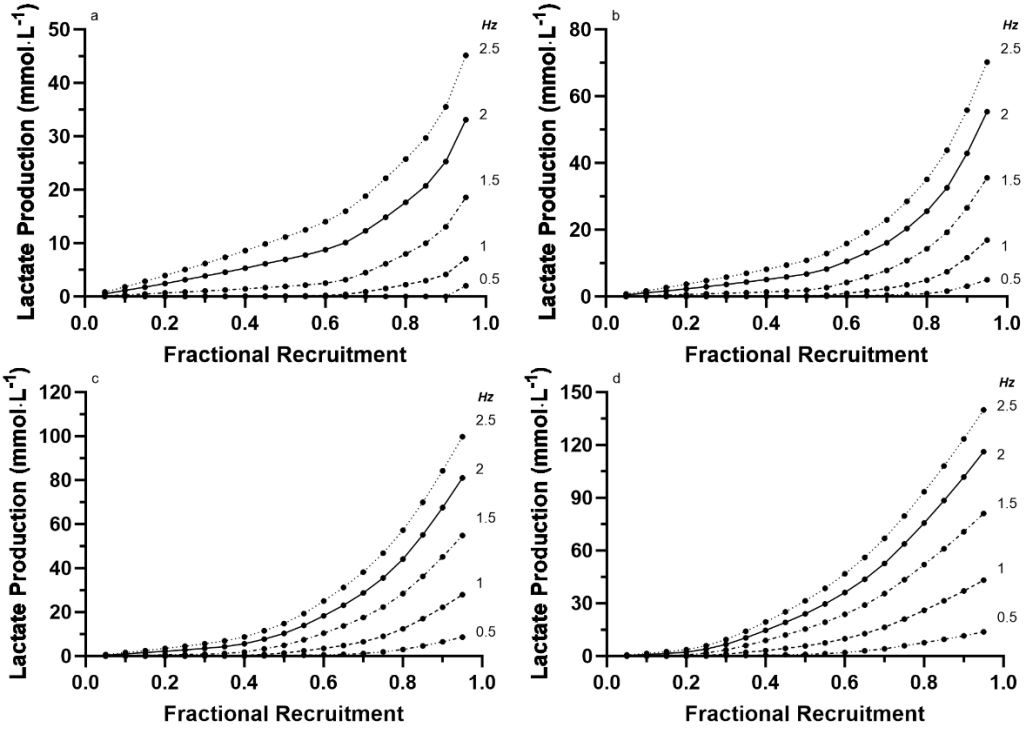

Figure 8: The lactate production across 0.05-0.95 fractional motor unit recruitment for 3 min of repeated contractions across 0.5 to 2.5 Hz, and genetic motor unit expressions (ST-FT) of a) 80-20, b) 60-40, c) 40-60, d) 20-80 %, respectively.

Discussion

Overall, substrate oxidation increased with increasing fractional motor unit recruitment and contraction frequencies, which is expected based on the first law of thermodynamics. The increasing substrate oxidation varied between the different ST-FT combinations and across different frequencies (0.5-2.5 Hz) as dictated by our predetermined dependency of contraction rate to profiles of percent contributions to ATP_{to} from the different metabolic systems (see Figure 2a-e). It is also important to note that the total range of exercise intensities covered in this model is non-physiologically extensive for 3 min of repeated contractions; contraction failure would occur in < 1 min for the repeated contractions at the higher end of motor unit recruitment. Nevertheless, this range provided an interesting analysis of the muscle contraction energy demands for motor unit recruitment that increase to near maximal. A detailed discussion of this issue will be presented later for each energy pathway.

During the 3 min of repeated contractions at 2.5 Hz and 95% fractional recruitment, the phosphagen system increased from 40 to 200 $mmol \cdot L^{-1}$ for the combined substrate phosphate transfer of the creatine kinase and adenylate kinase reactions for the genetic expressions of 80-20 vs 20-80 (%ST-FT), respectively (Figures 3 and 7). This upper value is substantial and differs from data and related assumptions inherent in prior research. This will be explained later in the Discussion.

The carbohydrate glycolytic energy system responded similarly to the phosphagen system increasing from 50 to 150 $mmol \cdot L^{-1}$ of glucose oxidation for the same genetic expressions and contractile conditions (Figures 5 and 7). This is lower than the phosphagen system, but as will be explained later, it is caused by the combination of the more complex involvement of the phosphagen system in contracting skeletal muscle across all exercise intensities, in combination with the differing ATP yields from the two pathways. The ATP yield from glucose is two (from blood glucose) to three-fold (from glycogen) more significant than for the phosphagen system (1.1 $mmol \cdot L^{-1}$ per $mmol \cdot L^{-1}$ substrate catalysis).

The carbohydrate mitochondrial respiration system differed considerably across contraction frequencies and fractional motor unit recruitment, but peak rates were similar in being close to 4 $mmol \cdot L^{-1}$ across all motor unit expression conditions (Figures 6 and 7). As will be

discussed later, the profile of carbohydrate oxidation across different contraction frequencies and fractional motor unit recruitment is complex due to the related complexity of the interaction between fatty acid and carbohydrate oxidation energy pathways (25) in addition to past errors in interpreting data of substrate oxidation from whole muscle, whole body or mixed fibre types of methods of research inquiry rather than at the cellular level specific to the different fibre types.

The profile for fatty acid oxidation is also complex as fatty acid oxidation was only prevalent during the low contraction frequency conditions. However, it was constrained after that due to increased carbohydrate oxidation associated with increasing FT motor unit recruitment (Figures 4 and 7). There is a large body of prior research on skeletal muscle fatty acid oxidation to compare and comment on, especially regarding the limitations of prior research in interpreting the cellular regulation of metabolism based on mixed muscle or whole methods. Nevertheless, based on the current model, the total fatty acid oxidation increased linearly for the 80-20 %ST-FT motor unit proportion condition for the 1 Hz contraction frequency and peaked at 0.373 $mmol \cdot L^{-1}$ at 95 % recruitment. This peak value was lower at 0.227 $mmol \cdot L^{-1}$ for the 20-80 % ST-FT condition at 0.5 Hz and 0.95 fractional motor unit recruitment. Such results clearly reveal the past errors of interpreting holistic measures of carbohydrate vs. fat oxidation to be solely caused by cellular regulation of muscle metabolism, as motor unit recruitment combined with increasing contraction frequencies are likely to be the main determinants of this transition in substrate oxidation.

A detailed discussion of these results will be provided below, structured by the need to understand the importance of the metabolic consequences and related regulation for how muscle fibres always contract maximally (All or None Principle), followed by details for each energy pathway.

Energy System Contributions During Exercise

The order of the energy systems will be based on fatty acid oxidation through mitochondrial respiration, the complete oxidation of carbohydrates (commencing with pyruvate) from mitochondrial respiration, carbohydrate oxidation in glycolysis resulting in lactate production (often referred to as anaerobic glycolysis), and finally the phosphagen system.

Fatty Acid - Mitochondrial Respiration

As previously stated, the peak FFA oxidation for the 3 min of repeated contractions was 0.373 mmol·L^{-1}. Romijn et al. (23) compared FFA to carbohydrate oxidation in six endurance trained cyclists during two conditions: a) normal fasting vs. b) continuous lipid and heparin (anti-coagulant) infusion during 30 min of cycling at 85 %VO_2max. As heparin detaches lipoprotein lipase from blood vessel walls, blood FFA concentrations increase further. The results from Romijn et al. (23) for FFA-MR were 26.7 vs. 34 μmol·kg^{-1} body mass·min^{-1}, for the normal vs. infusion conditions, respectively. The unit conversion from kg body mass to L muscle water which pertained to the model results is difficult, but as the subjects' mean weight was 75.8 kg, and if we assume a lean body mass of 85% of which muscle was 70%, an active muscle mass of 20 kg, and a conversion from muscle mass to muscle water of 1.37, the prior results convert to values of 82.49 vs. 106.44 μmol·L^{-1}·min^{-1}, respectively. For the 30 min duration, these rates now total 2.475 vs. 3.193 mmol·L^{-1}, respectively.

The comparison to the peak rate from the model for 80-20 %ST genetic expression and 1 Hz rate of contractions of 0.373 mmol·L^{-1} must be understood to be from one muscle for 3 min of repeated contractions, and as such, the value should be dramatically lower than the results of Romijn et al. (23). This comparison proves interesting because, based on an exercise time correction alone, the result from the model would increase to 3.73 mmol·L^{-1}. This value is comparable to the highest (lipid and heparin infusion) condition of the Romijn et al. (23) study. Given the assumptions made to compare the whole-body data of Romijn et al. (23) to the single pure muscle data of the model, the results seem to have physiological relevance.

An added comparison of the model data can be obtained from the research of Coggan et al. (20). In that study, a comparison between untrained and trained subjects was made for fatty acid oxidation when cycling at 75% of VO_2max. When employing the same conversion strategy that was applied for the Romijin et al. (23) study, total fatty acid oxidation for the untrained vs trained subjects equated to 3 min of exercise calculated to be 0.072 vs. 0.175 mmol·L^{-1}, respectively. Interestingly, the results from Coggan et al. (20), for the trained subjects were approximately half that of the Romijin et al. (23) study. However, note that the higher numbers for the Romijin et al. (23) study were likely caused by the added blood FFA concentrations resulting from the heparin infusion. Based on the results from the model, this

compares favourably to the 80-20 %ST-FT, 1 Hz and 30 % fractional motor unit recruitment, which was 0.131 mmol·L^{-1}.

Carbohydrate Oxidation

It was difficult to compare results from prior research of carbohydrate oxidation to the data from the model. The core problem is that no prior research has been able to divide total carbohydrate oxidation into separate values for mitochondrial respiration vs. glycolysis. As such, comparisons will be made to prior research on whole-body exercise for total carbohydrate oxidation, with added comparison of research estimates of anaerobic glycolytic carbohydrate oxidation and lactate production.

Whole-body exercise

Most prior research on carbohydrate oxidation during exercise involved whole body exercise of low to moderate exercise intensities or high intensity exercise to ascertain muscle anaerobic capacities and related glycolytic contributions. In either case, as for the discussion of fatty acid oxidation, there are many assumptions to make when recalculating whole body data to muscle data. For the Romijn et al. study (23), data retrieved for whole body carbohydrate oxidation equated to 259 μmol·kg^{-1} body mass·min^{-1} for cycling exercise at 85% VO_2max. Adjusting for a total muscle mass of 45.1 kg and 20 kg of exercised muscle mass, further corrected to muscle water and 3 min of exercise, this converts to a total of 2.4 mmol·L^{-1}. For comparing this result to those of the model, the difficulty lay in appropriating the exercise intensity of the Romijn et al. (23) study to fractional motor unit recruitment. The subjects of the Romijn et al. (23) study, were highly endurance trained athletes who were able to remain at a steady state for this intensity. Thus, using the data from the model for 80-20 %ST-FT proportions, and an assumed 30% motor unit recruitment for repeated contractions at 1 Hz, this amounted to a combined total from carbohydrate glycolytic and mitochondrial respiration of 0.22 mmol·L^{-1} (0.14 + 0.08 mmol·L^{-1} for glycolysis and mitochondrial respiration, respectively.

Interestingly, when using the modelled data for 20-80 %ST-FT proportions at 1 Hz, 30 % motor unit recruitment retrieves a value of 1.74 mmol·L^{-1} for total carbohydrate oxidation. When motor unit recruitment is increased to 35% of total carbohydrate oxidation increases to 3.03 mmol·L^{-1}. The data from the model documents the importance of the muscle fibre type contributions to muscle metabolism during exercise and the resultant substrate oxidation.

This is a significant contribution the model provides to understanding the balance of different substrate oxidation in contracting skeletal muscle.

Glycolysis and Lactate Production

Lactate production was calculated as the difference between glycolytic and mitochondrial carbohydrate oxidation. The data for muscle lactate production (Figure 8) ranged from 2 to 140 $mmol \cdot L^{-1}$ for 80-20 %ST-FT and 0.5 Hz contractions vs. 20-80 %ST-FT and 2.5 Hz contractions. This extensive range and peak data for lactate production exceeded prior measured values in muscle for 2 to 3 min of electrically stimulated intense muscle contractions to contractile failure, being 145 $mmol \cdot kg^{-1}$ dry weight = 46.2 $mmol \cdot L^{-1}$ muscle water (24). This is expected, for prior research has assumed that ensuring zero limb blood flow means that muscle lactate concentrations can be interpreted as the total capacity of muscle lactate production. This is not logical, for even in a limb compressed with a tourniquet, muscle lactate would equilibrate between intracellular and extracellular fluid and the tissue mass that it is cleared by. This then requires an inflation of estimates of muscle lactate production due to the expanse of the fluid space for lactate distribution beyond the muscle mass it originates from. For example, assume a resting muscle and blood lactate of 1 $mmol \cdot L^{-1}$, a post-exercise muscle lactate value of 40 $mmol \cdot L^{-1}$, and an entire dilution water volume of the thigh of 3 L. Adjusting for all factors equates to 120 $mmol \cdot L^{-1}$ of lactate production. This is remarkably close to the highest data calculated in the model, as shown in Figure 8d.

Phosphagen (CK-AK) System

The phosphagen system primarily involves the creatine kinase reaction and the adenylate kinase reaction, which have been largely misunderstood for over a century. This is because the overwhelming and continued interpretation of the system has been that it is only involved during more intense muscle contractions and, as such, coincides with exercise conditions leading to the rapid onset of contractile failure and related volitional exhaustion. This can be seen in numerous research studies of this system during the mid-to-late 20th century (4,22,24,26).

Research of the creatine kinase shuttle proposed a revised approach to interpreting the role of the phosphagen system during repeated muscle contractions across all exercise intensities (19). This interpretation proposed that the creatine kinase and adenylate kinase reactions were involved in free energy transfer from mitochondrial ATP regeneration to the cytosol. This

theory implied (at that time, it did not provide evidence) that such reactions were crucial for rapid free energy transfer during low and more intense muscle contractions. A logical hypothesis from this theory would be that if this was true, then there should be evidence of decreasing creatine phosphate concentrations, even though minor, during low intensity muscle contractions.

In the late 1900s, Haseler et al. (21) and Hogan et al. (27) provided this information and dramatically changed how the phosphagen system is interpreted. The most compelling evidence was from Haseler et al. (21), who revealed significant decreases (to 62% of rest) in muscle CrP concentrations during 10 min of repeated contractions of the calf muscle at 1 Hz at 60% (7.2 Watts) of peak power. Such exercise was completed with muscle pH remaining above 7.04. The core interpretation of this research as an extension of the creatine kinase shuttle was that creatine phosphate was repeatedly used to regenerate cytosolic ATP and nearly simultaneously be partially replenished based on mitochondrial respiration, even during low to moderate intensity exercise. Even though this research did not factor into their interpretations of the complexities of motor unit recruitment, in addition to the different involvement of the two muscles (gastrocnemius and soleus) that have two genetically divergent motor unit proportion expressions (the soleus expressed more to slow twitch dominance), the results supported the creatine kinase shuttle theory.

The assumed data of Figure 2 included this interpretation of the CK-AK system, where the involvement of the CK-AK system reactions was evident across all rates of muscle contractions of the VL, though increasing as a non-linear function. Such evidence documents that it is an over-simplification to view decreases in muscle creatine phosphate concentrations during exercise as a valid measure of absolute involvement in free energy transfer. The muscle concentration of creatine phosphate is a dynamic balance between breakdown and regeneration. This is best seen in Figure 3a, where the total recruited muscle fibres during repeated contractions at 1.5 Hz reveal an approximate 12 $mmol \cdot L^{-1}$ combined (creatine phosphate and adenylate kinase reactions) contribution to free energy transfer. The involvement of the CK-AK system for values in excess of 12 $mmol \cdot L^{-1}$ can be explained by the balance of the regeneration and breakdown resulting in higher net absolute involvement and partial recovery of creatine phosphate in the rest intervals between contractions, thereby

adding to total net involvement over time, and the non-physiological conditions of high motor unit recruitment sustained for 3 min (see Limitations).

Perspectives and Significance

This research is unique as it is a computational model. It is important to know from a fibre type perspective the implications of an improved understanding of muscle metabolism during exercise of different intensities. Furthermore, it is vital to consider the rates of contraction concerning the All or None Principle. There may be an optimal frequency at which energy systems are most efficiently utilised. The results highlight muscle metabolism during different exercise intensities but also suggest how the rate of contractions, governed by the All or None Law, plays a role in utilising energy during muscle activity. This understanding can better inform training strategies to optimise the health and performance of an individual. Currently, there needs to be more research on fibre type specific substrate oxidation, which made it difficult to compare the results of this paper.

Limitations

Limitations of the data include the prior research, which consisted of whole muscle samples from human or animal samples. As such, the change in proportionality for contraction frequencies was based on theoretical models and not data acquired from experimental research (this cannot be done with current technology). This research only used one muscle, the vastus lateralis with five known muscle fibre types (Type, I-IIa, IIa, IIab and IIb). When comparing the data to other studies, this caused some difficulty as the prior research used whole muscle samples, which consisted of a mixed fibre type and not individual fibre types. It was also assumed that muscle contractile function wasn't impaired due to metabolic causes of contractile failure with increasing motor unit recruitment and during the increasing duration of the 3 min exercise condition. We assumed that metabolic efficiency was constant across the exercise condition and each of the fibre types when calculating the data. All the prior limitations might compromise the accuracy and validity of the data. Thus, it is essential to consider these when analysing the results.

Conclusions and Recommendations

The model proved that single muscle fibre contractile power, and how it varies between fibre types, can be transferred to quantifying cellular bioenergetics based on the first law of thermodynamics. Such cellular capacities can then be summed to yield total energy exchange data that is remarkably close to measures of mixed muscle fibre type sampling that yield estimates of whole muscle metabolism. The quantification of substrate oxidation turnover has relevance to sporting contexts and to neuromuscular diseases that alter cellular metabolism.

The model's results have the potential to stimulate further research, which could significantly improve the model and the related data produced. This, in turn, would enhance our understanding of the roles of motor unit (fibre type) specific attributes and their suitability (or not) for specific movement/exercise demands. The implications of this could be far-reaching, particularly in the fields of sports science and neuromuscular diseases.

References

1. Bottinelli R, Canepari M, Pellegrino MA, Reggiani C. Force-velocity properties of human skeletal muscle fibres: myosin heavy chain isoform and temperature dependence. Journal Physiol 1996;495(2):573–586. https://doi.org/10.1113/jphysiol.1996.sp021617
2. Edgerton VR, Smith JL, Simpson DR. Muscle fibre type populations of human leg muscles. Histochem J 1975;7(3):259–266. https://doi.org/10.1007/BF01003594
3. Gollnick PD, Piehl K, Saltin B. Selective glycogen depletion pattern in human muscle fibres after exercise of varying intensity and at varying pedalling rates. Journal Physiol 1974;241(1):45–57. https://doi.org/10.1113/jphysiol.1974.sp010639
4. Tesch PA, Colliander EB, Kaiser P. Muscle metabolism during intense, heavy-resistance exercise. Eur J Appl Physiol Occup Physiol 1986;55(4):362–366. https://doi.org/10.1007/BF00422734
5. Lexell J, Henriksson-Larsén K, Winblad B, Sjöström M. Distribution of different fiber types in human skeletal muscles: Effects of aging studied in whole muscle cross sections. Muscle & Nerve 1983;6(8):588–595. https://doi.org/10.1002/mus.880060809
6. Trappe, S., Gallagher, P., Harber, M., Carrithers, J., Fluckey, J., & Trappe, T. Single muscle fibre contractile properties in young and old men and women. Journal Physiology 2003;552(Pt 1):47–58. https://doi.org/10.1113/jphysiol.2003.044966
7. Schiaffino, S., & Reggiani, C. Fiber types in mammalian skeletal muscles. Physiol Rev 2011;91(4):1447–1531. https://doi.org/10.1152/physrev.00031.2010
8. Bottinelli, R. Functional heterogeneity of mammalian single muscle fibres: Do myosin isoforms tell the whole story? Pflügers Archiv 2001;443(1):6–17. https://doi.org/10.1007/s004240100700
9. Termin A, Staron RS, Pette D. Myosin heavy chain isoforms in histochemically defined fiber types of rat muscle. Histochemistry 1989;92(6):453–457. https://doi.org/10.1007/BF00524756
10. Brooke MH, Kaiser KK. Three human myosin ATPase systems and their importance in muscle pathology. Neurology 1970;20(4):404–405.

11. Andreassen S, Arendt-Nielsen L. Muscle fibre conduction velocity in motor units of the human anterior tibial muscle: a new size principle parameter. J Physiol 1987;391(1):561–571. https://doi.org/10.1113/jphysiol.1987.sp016756
12. Burke RE, Tsairis P. Anatomy and innervation ratios in motor units of cat gastrocnemius. The Journal of Physiology 1973;234(3):749–765. https://doi.org/10.1113/jphysiol.1973.sp010370
13. Henneman E. Relation between size of neurons and their susceptibility to discharge. Science 1957;126(3287):1345–1347. https://doi.org/10.1126/science.126.3287.1345
14. Hall JE. Guyton & Hall Physiology Review (3rd ed.). 2015, Elsevier Health Sciences.
15. Marcucci L, Reggiani C, Natali AN, Pavan PG. From single muscle fiber to whole muscle mechanics: a finite element model of a muscle bundle with fast and slow fibers. Biomechanics and modeling in mechanobiology 2017;16(6):1833–1843. https://doi.org/10.1007/s10237-017-0922-6
16. Mulligan L, Nygaard G, Holland J, Robergs R. Modelling Skeletal Muscle Motor Contributions to Contractile Function: Part 1 - Velocity, Force and Power. Qeios 2024; htttps://doi:10.32388/VREACR
17. Davies, J., Nygaard, G., Holland, J., Robergs, R. Modelling Skeletal Muscle Motor Contributions to Contractile Function: Part 2 – Total (aerobic + anaerobic) ATP Turnover. Qeios 2024; Qeios. doi:10.32388/QF5FI0.
18. He Z-H, Bottinelli R, Pellegrino MA, Ferenczi MA, Reggiani C. ATP Consumption and Efficiency of Human Single Muscle Fibers with Different Myosin Isoform Composition. Biophysical Journal 2000;79(2):945–961. https://doi.org/10.1016/S0006-3495(00)76349-1
19. Bessman SP, Carpenter CL. The creatine-creatine phosphate energy shuttle. Annual Rev Biochem 1985;54:831–862. https://doi.org/10.1146/annurev.bi.54.070185.004151
20. Coggan AR, Raguso CA, Gastaldelli A, Sidossis LS, Yeckel CW. Fat metabolism during high-intensity exercise in endurance-trained and untrained men. Metabolism: clinical and experimental, 2000;49(1):122–128. https://doi.org/10.1016/s0026-0495(00)90963-6

21. Haseler LJ, Richardson RS, Videen JS, Hogan MC. Phosphocreatine hydrolysis during submaximal exercise: the effect of FIO2. J Appl Physiology 1998;85(4):1457–1463. https://doi.org/10.1152/jappl.1998.85.4.1457
22. McCartney N, Spriet LL, Heigenhauser GJ, Kowalchuk JM, Sutton JR, Jones NL. Muscle power and metabolism in maximal intermittent exercise. J Applied Physiol 1986;60(4):1164–1169. https://doi.org/10.1152/jappl.1986.60.4.1164
23. Romijn JA, Coyle EF, Sidossis LS, Zhang XJ, Wolfe RR. Relationship between fatty acid delivery and fatty acid oxidation during strenuous exercise. J Applied Physiol 1995;79(6):1939–1945. https://doi.org/10.1152/jappl.1995.79.6.1939
24. Spriet LL, Söderlund K, Bergström M, Hultman E. Anaerobic energy release in skeletal muscle during electrical stimulation in men. J Applied Physiol 1987;62(2):611–615. https://doi.org/10.1152/jappl.1987.62.2.611
25. Spriet LL. New insights into the interaction of carbohydrate and fat metabolism during exercise. Sports Med 2014;44(Suppl 1):S87–S96. https://doi.org/10.1007/s40279-014-0154-1
26. Knuttgen HG, Saltin B. Muscle metabolites and oxygen uptake in short-term submaximal exercise in man. J Applied Physiol 1972;32(5):690–694. https://doi.org/10.1152/jappl.1972.32.5.690
27. Hogan MC, Richardson RS, Haseler LJ. Human muscle performance and PCr hydrolysis with varied inspired oxygen fractions: a 31P-MRS study. J Applied Physiol 1999;86(4):1367–1373. https://doi.org/10.1152/jappl.1999.86.4.1367